

## Supplementary materials

### Inorganic-organic Hybrid Compounds Based on Novel Lanthanide-Antimony Oxohalide Nanoclusters

Bing Hu,<sup>a</sup> Guo-Dong Zou,<sup>a,b</sup> Mei-Ling Feng<sup>a</sup> and Xiao-Ying Huang<sup>\*a</sup>

<sup>a</sup>State Key Laboratory of Structural Chemistry, Fujian Institute of Research on the Structure of Matter, the Chinese Academy of Sciences, Fuzhou, Fujian 350002, P.R. China

<sup>b</sup>Graduate University of the Chinese Academy of Sciences, Beijing 100049, P. R. China

Fax: +86 591 83793727; Tel: +86 591 83793727; E-mail: [xyhuang@fjirsm.ac.cn](mailto:xyhuang@fjirsm.ac.cn)

#### 1. X-ray crystallographic study

Single crystal X-ray diffraction was performed on an Oxford Xcalibur Eos CCD diffractometer with graphite-monochromated MoK $\alpha$  radiation ( $\lambda = 0.71073 \text{ \AA}$ ) at room temperature. The data were corrected for Lorentz and polarization effects as well as for absorption. The structures were solved by direct methods using SHELXS-97<sup>1</sup> and refined by full-matrix least-squares procedure on  $F^2$  with SHELXL-97. Some of the C, O and N atoms in the 1,10-phen, 2-MepyH and TDC ligands in compound **1** were refined with 667 restraints (DFIX, SIMU, DELU and ISOR) to obtain the chemical-reasonable models and reasonable atomic displacement parameters. In compound **1**, there still exist a few large isolated residual density peaks ( $< 2.233 \text{ e\AA}^{-3}$ ) in the difference Fourier-maps that should be assigned for the oxygen atoms of highly disordered lattice water molecules. However, it was difficult to locate all the disordered water molecules according to the D-F maps. Therefore, finally only one lattice water molecule per asymmetric unit was added and refined. The empirical formula of **1** was determined to include 20 water molecules according to the EA and TGA analyses. In compound **2**, 1219 restraints (DFIX and SIMU) were applied for some of the C and N atoms in the 2-MepyH cations so that their bond geometries and atomic displacement parameters were reasonable. A few large residual density peaks ( $< 1.693 \text{ e\AA}^{-3}$ ) are present close to the metal atoms due to the smearing effect of the heavy metals which shows no feature.

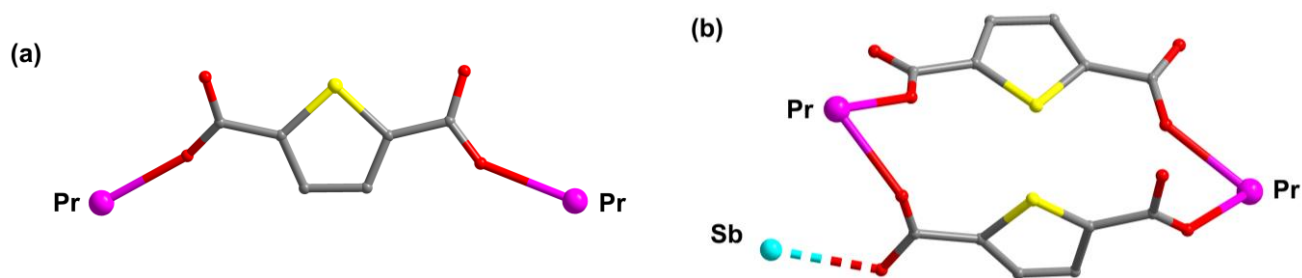


Fig. S1 Coordination modes of three TDC ligands in the asymmetry unit in compound **1**.

## 2. More Characterizations

Powder X-ray diffraction (PXRD) patterns were recorded on a Rigaku Miniflex II diffractometer using  $\text{CuK}\alpha$  radiation. C, H and N analyses were performed on a German Elementary Vario EL III instrument. IR spectrum was recorded on a Magna 750 FT-IR spectrometer photometer as KBr pellets in the range of  $4000\sim 450\text{ cm}^{-1}$ . Thermogravimetric (TG) analyses were carried out with a NETZSCH STA 449C unit at a heating rate of  $10\text{ }^\circ\text{C}/\text{min}$  under a nitrogen atmosphere. Optical diffuse reflectance spectra were measured at room temperature with a Perkin-Elmer Lambda 900 UV/Vis spectrophotometer. A  $\text{BaSO}_4$  plate was used as a standard (100% reflectance). The absorption spectrum was calculated from reflectance spectrum by using the Kubelka–Munk function:  $a/S=(1-R)^2/2R$ , where  $a$  is the absorption coefficient,  $S$  is the scattering coefficient which is practically independent of wavelength when the particle size is larger than  $5\text{ }\mu\text{m}$ , and  $R$  is the reflectance. Photoluminescence spectrum was recorded on a Perkin-Elmer LS 55 luminescence spectrometer with a R928 red-sensitive photomultiplier without correction.

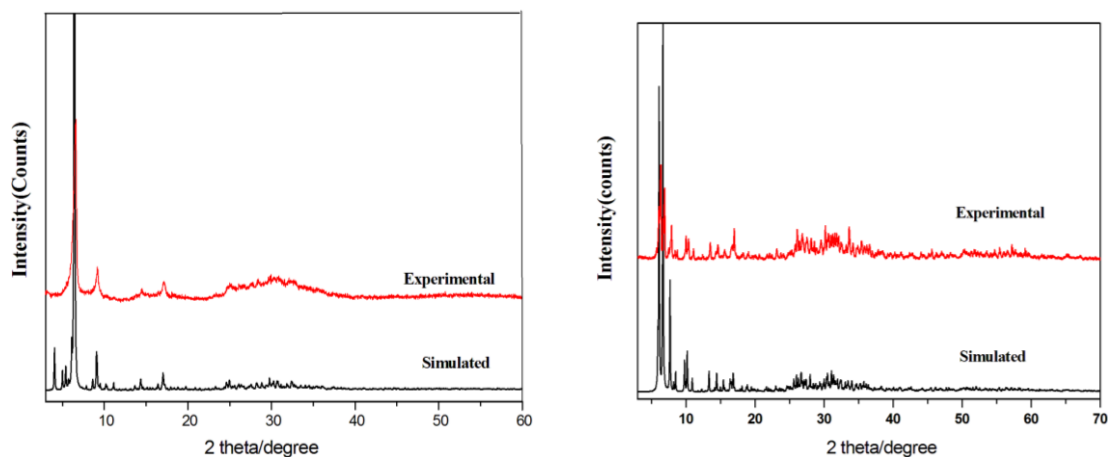


Fig. S2 Comparison of the powder X-ray diffraction patterns of compounds **1** (left) and **2** (right) with that simulated from the single-crystal X-ray diffraction data (bottom).

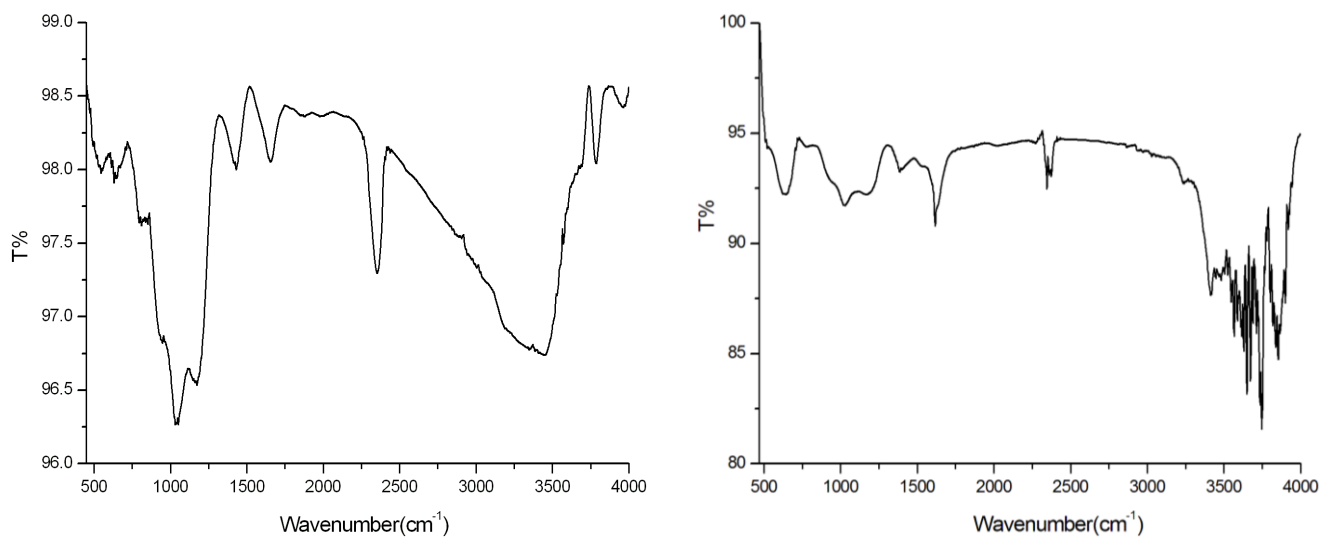


Fig. S3 IR Spectra of **1** (left) and **2** (right).

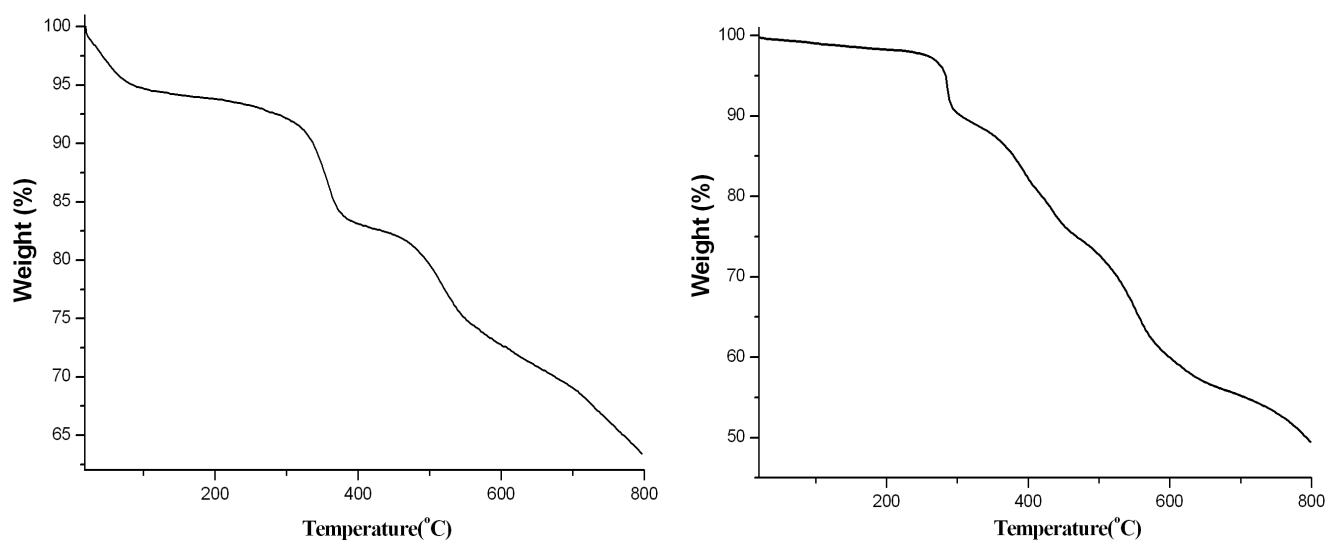


Fig. S4 TG curve of compounds **1** (left) and **2** (right).

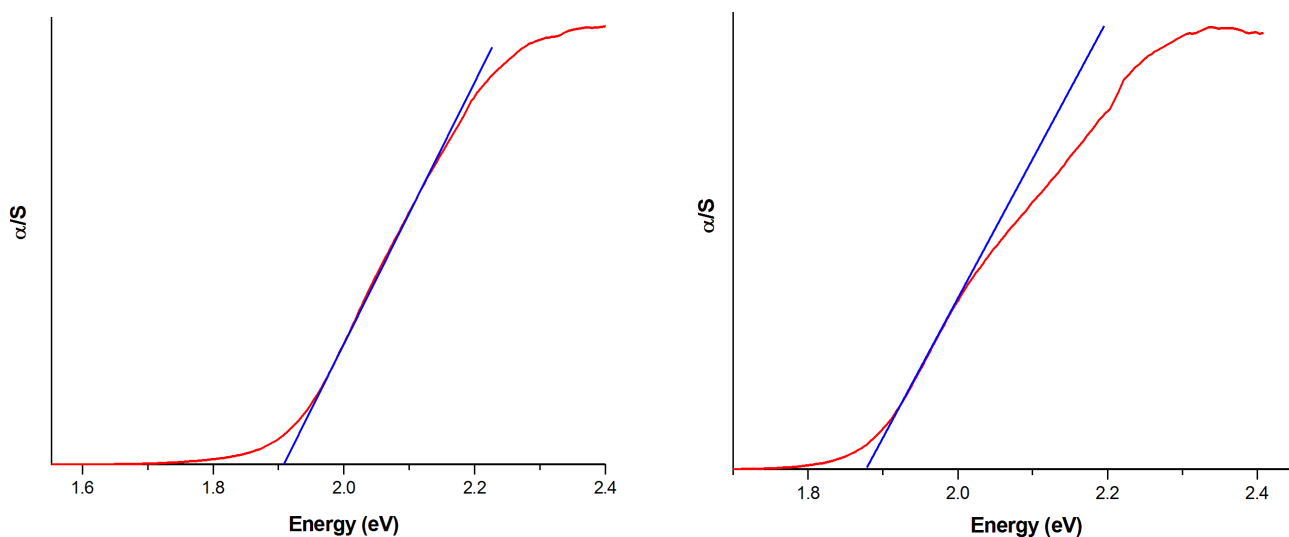


Fig. S5 Variations of  $(\alpha h\nu)^{1/2}$  as function of photon energy for **1** (left) and **2** (right).

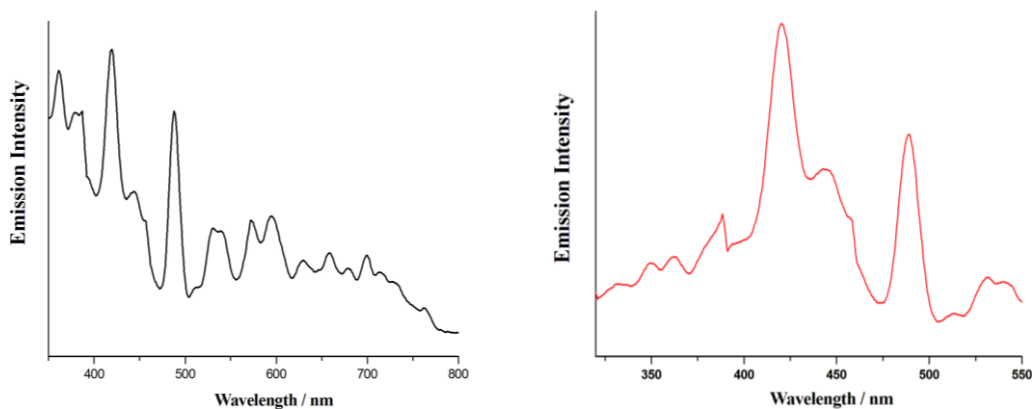


Fig. S6 Solid-state emission spectra of compounds **1** (left) and **2** (right).

### 3. More structural Figures

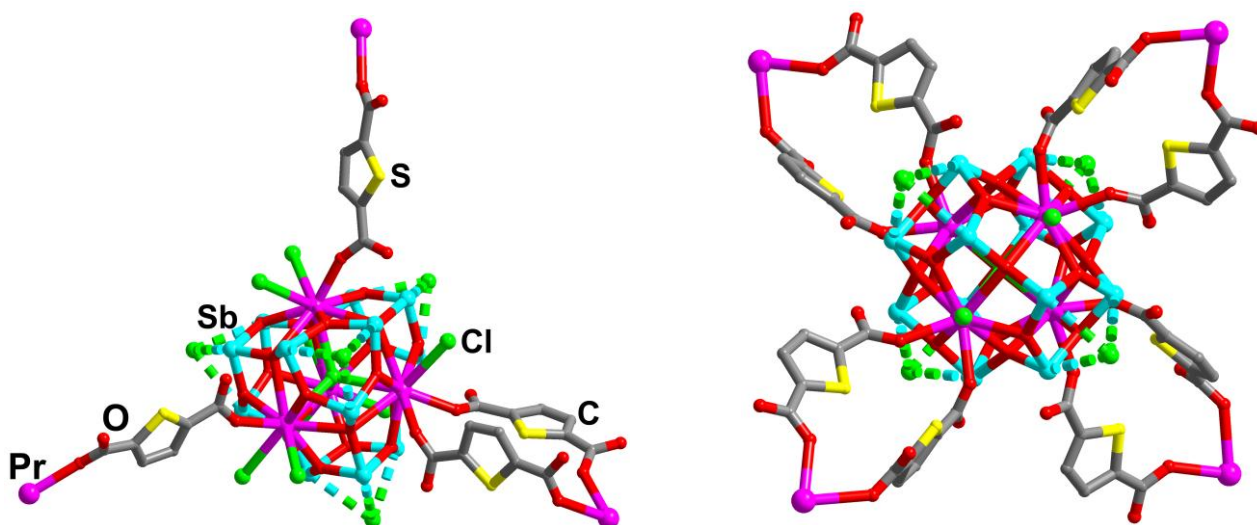


Fig. S7 Clusters **A** (left) and **B** in **1**.

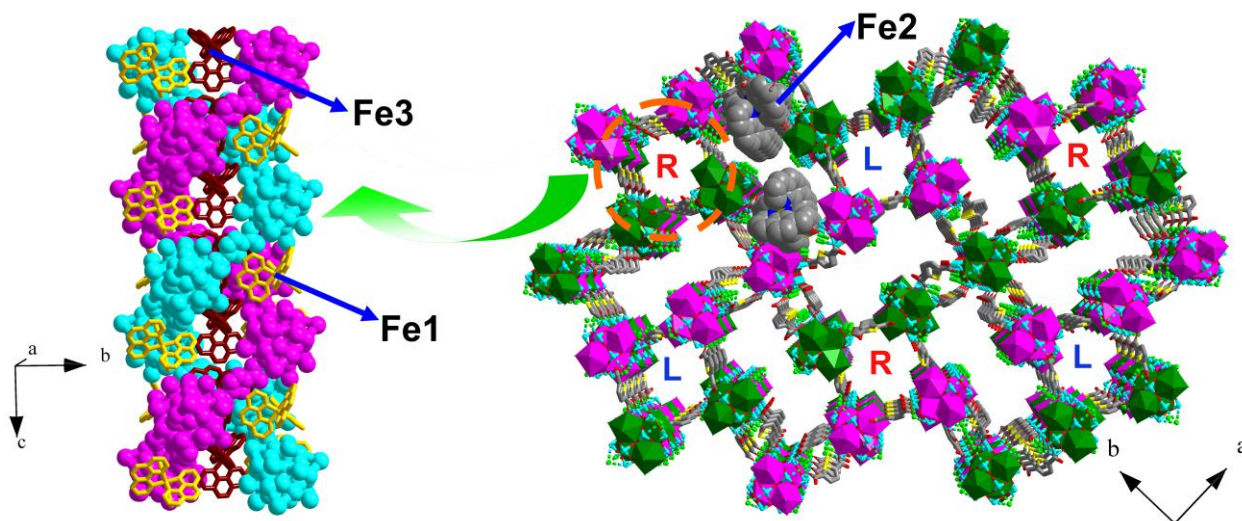


Fig. S8 Prospective view of the two-fold interpenetrating anionic network of **1** (right) along the *c*-axis and a fragment of the double-helical chains (left) along the *c*-axis, with the [Fe(1,10-phen)<sub>3</sub>] cations labeled.

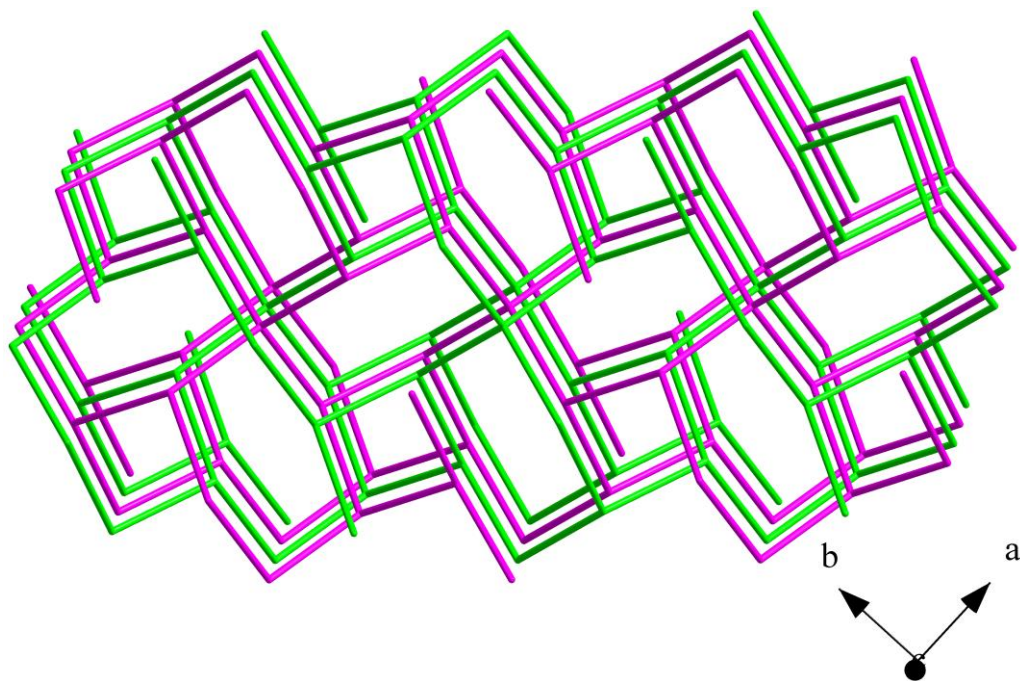


Fig. S9 Topological view of the two-fold interpenetrating nets in **1**.

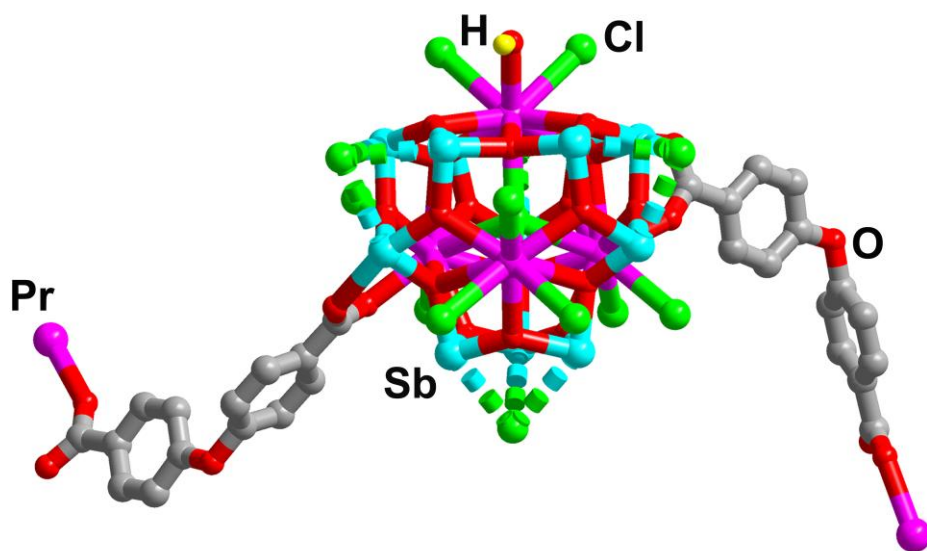


Fig. S10  $[\text{Pr}_4\text{Sb}_{12}\text{O}_{18}(\text{OH})\text{Cl}_{14}]$  cluster in **2**.